Journal List > Proc Natl Acad Sci U S A > v.105(1); Jan 8, 2008

Proc Natl Acad Sci U S A. 2008 January 8; 105(1): 106–111. PMCID: PMC2224167
Published online 2007 December 26. doi: 10.1073/pnas.0707892105.

Biochemistry

p53 and TFIIEα share a common binding site on the Tfb1/p62 subunit of TFIIH

Paola Di Lello,[*] Lisa M. Miller Jenkins,[†] Caroline Mas,[*] Chantal Langlois,[*] Elena Malitskaya,[*] Amélie Fradet-Turcotte,[‡] Jacques Archambault,[‡] Pascale Legault,[*] and James G. Omichinski[*§]

*Département de Biochimie, Université de Montréal, C.P. 6128 Succursale Centre-Ville, Montréal, QC, Canada H3C 3J7;
[†]Laboratory of Cell Biology, National Cancer Institute, National Institutes of Health, 37 Convent Drive, Bethesda, MD 20892-4256; and
[‡]Institut de Recherches Cliniques de Montréal, 110 Avenue des Pins Ouest, Montréal, QC, Canada H2W 1R7
[§]To whom correspondence should be addressed. E-mail: jg.omichinski@umontreal.ca
Edited by Gary Felsenfeld, National Institutes of Health, Bethesda, MD, and approved November 14, 2007
Contributed by
Author contributions: P.D.L., L.M.M.J., J.A., P.L., and J.G.O. designed research; P.D.L., L.M.M.J., C.M., C.L., E.M., A.F.-T., J.A., P.L., and J.G.O. performed research; P.D.L., C.M., C.L., E.M., A.F.-T., J.A., and J.G.O. contributed new reagents/analytic tools; P.D.L., L.M.M.J., E.M., J.A., P.L., and J.G.O. analyzed data; and P.D.L., J.A., P.L., and J.G.O. wrote the paper.

Received August 21, 2007

ABSTRACT

The general transcription factor IIH is recruited to the transcription preinitiation complex through an interaction between its p62/Tfb1 subunit and the α-subunit of the general transcription factor IIE (TFIIEα). We have determined that the acidic carboxyl terminus of TFIIEα ($TFIIE\alpha_{336–439}$) directly binds the amino-terminal PH domain of p62/Tfb1 with nanomolar affinity. NMR mapping and mutagenesis studies demonstrate that the TFIIEα binding site on p62/Tfb1 is identical to the binding site for the second transactivation domain of p53 (p53 TAD2). In addition, we demonstrate that $TFIIE\alpha_{336–439}$ is

capable of competing with p53 for a common binding site on p62/Tfb1 and that TFIIEα$_{336–439}$ and the diphosphorylated form (pS46/pT55) of p53 TAD2 have similar binding constants. NMR structural studies reveal that TFIIEα$_{336–439}$ contains a small domain (residues 395–433) folded in a novel ββαααα topology. NMR mapping studies demonstrate that two unstructured regions (residues 377–393 and residues 433–439) located on either side of the folded domain appear to be required for TFIIEα$_{336–439}$ binding to p62/Tfb1 and that these two unstructured regions are held close to each other in three-dimensional space by the novel structured domain. We also demonstrate that, like p53, TFIIEα$_{336–439}$ can activate transcription *in vivo*. These results point to an important interplay between the general transcription factor TFIIEα and the tumor suppressor protein p53 in regulating transcriptional activation that may be modulated by the phosphorylation status of p53.

Keywords: NMR, phosphatidylinositol 5-phosphate, transcription regulation, activation domains, isothermal titration calorimetry

In eukaryotic cells, a crucial event for the transcription cycle of protein-coding genes is the assembly of RNA polymerase II (RNAP II) and the general transcription factors at the DNA promoter region to form the preinitiation complex (PIC) (1, 2). According to the sequential assembly model of the PIC formation, the last steps in transcription initiation are the binding of the general transcription factor IIE (TFIIE) to the PIC, followed by the TFIIE-assisted recruitment of the general transcription factor IIH (TFIIH) (3, 4). The association of TFIIE and TFIIH to the initial PIC is essential for RNAP II to proceed from an unphosphorylated form to a phosphorylated form and also for the transition from the initiation to the elongation phase of transcription (5, 6).

TFIIE is composed of two subunits, α and β. The larger α-subunit (TFIIEα) contains several functional domains that are mainly located at the amino-terminal half of the protein. These domains have been demonstrated to be critical for basal transcription and cell growth (7, 8), and they are required for the interaction of TFIIEα with the β-subunit of TFIIE (TFIIEβ), RNAP II, and other transcription factors, as well as for regulating the enzymatic activities of TFIIH (4, 7, 9). TFIIEβ also possesses functional domains that are responsible for important interactions with TFIIEα, RNAP II, TFIIB, and TFIIF

(10).

Human TFIIH (factor b in yeast) is composed of 10 subunits divided in two complexes, the core TFIIH (XPB, p62, p52, p44, p34, and TTDA in humans and Ssl2, Tfb1, Tfb2, Ssl1, Tfb4, and Tfb5 in yeast) and the CAK complex (cdk7, cyclin H, and MAT1 in humans and Kin28, Ccl1, and Tfb3 in yeast). TFIIH has three enzymatic activities (DNA-dependent ATPase, ATP-dependent helicase, and CTD kinase) that are essential at various stages of transcription initiation and elongation. The XPB helicase is required for the formation of an open complex during transcription initiation and is also implicated in promoter clearance (11), whereas the kinase cdk7 is responsible for the phosphorylation of the carboxyl-terminal domain (CTD) of the largest subunit of RNAP II (12). Phosphorylation of the CTD allows RNAP II to progress from the initiation phase to the elongation phase of transcription (13).

The functions of TFIIE and TFIIH are tightly correlated and reciprocally regulated. In fact, it has been observed that TFIIEα not only is involved in recruiting TFIIH to the PIC but can also stimulate the ATPase and kinase activities and repress the helicase activity of TFIIH (3, 9, 14). On the other hand, TFIIH is able to phosphorylate TFIIEα, and this phosphorylation has been postulated to affect the interaction between TFIIE and other proteins involved in either basal or activated transcription initiation (9, 15).

In vivo and *in vitro* studies have demonstrated that TFIIE and TFIIH bind directly to each other through an interaction involving the highly acidic carboxyl terminus of TFIIEα and the p62/Tfb1 subunit of TFIIH (7, 16). In addition, the p62/Tfb1 subunit has been shown to interact with a number of acidic transactivation domains (TADs) including the second TAD of p53 (p53 TAD2). The interaction between p53 TAD2 and p62/Tfb1 is enhanced by phosphorylation of Ser-46 and Thr-55 of p53. This interaction between p62/Tfb1 and p53 TAD2 is thought to be important for regulation of selected p53-regulated genes that require p53 TAD2, such as MDM2, PUMA, WAF1, and BAX1 (17, 18).

In this article we use isothermal titration calorimetry (ITC), NMR spectroscopy, and site-directed mutagenesis experiments to define the molecular basis of the interaction between TFIIEα and the p62/Tfb1 subunit of TFIIH. In addition, we identified a domain within the carboxyl terminus of

TFIIEα, and we demonstrate that TFIIEα and the transactivation domain of the tumor suppressor protein p53 can compete for a common binding site on p62/Tfb1.

RESULTS AND DISCUSSION

TFIIEα Binds the PH Domain of p62.

$TFIIE\alpha_{336–439}$ is extremely acid-rich because it contains a high proportion of aspartic acid and glutamic acid residues (36.5%; 38 of 104 residues). In addition, $TFIIE\alpha_{336–439}$ has a significant number of hydrophobic residues, and this acidic/hydrophobic sequence composition bears similarity to the amino acid composition found in the TADs of a number of transcriptional activator proteins including p53, NFκB, GCN4, Gal4, and VP16. We have previously demonstrated that the TADs of VP16 and p53 bind to the PH domain of the p62/Tfb1 (human/yeast) subunit of TFIIH (19, 20). Because the carboxyl terminus of TFIIEα interacts with the p62/Tfb1 subunit of TFIIH (7, 16) and has an amino acid composition (acidic/hydrophobic) similar to the TADs of VP16 and p53, we used ITC to determine whether $TFIIE\alpha_{336–439}$ would also bind to the PH (pleckstrin homology) domain of p62. ITC studies demonstrated formation of a $p62_{1–127}$/$TFIIE\alpha_{336–439}$ complex, and the dissociation constant (K_d) was determined to be 45 ± 25 nM (Table 1). The affinity of $TFIIE\alpha_{336–439}$ for $p62_{1–127}$ is almost two orders of magnitude stronger than the K_d for the $p62_{1–127}$/p53 complex (3,175 ± 570 nM) (20). However, the K_d for the $p62_{1–127}$/$TFIIE\alpha_{336–439}$ complex is very similar to the one determined for the complex between p62 and a diphosphorylated form of p53 (pS46/pT55), which has a K_d of 97 ± 33 nM (20).

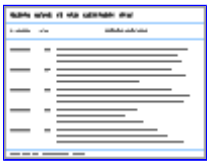

Table 1.
Dissociation constants, K_d, for the binding of the carboxyl terminus of TFIIEα to the PH domain of p62 in 20 mM Tris at pH 7.5 as determined by ITC

Once we had verified the formation of a complex involving $p62_{1–127}$ and $TFIIE\alpha_{336–439}$, we performed NMR chemical shift mapping studies to define the binding site of $TFIIE\alpha_{336–439}$ on the PH domain of Tfb1 ($Tfb1_{1–115}$). The amino-terminal PH domains of human p62 and yeast Tfb1 are structurally and functionally very similar, and we have previously shown that the PH domain of Tfb1 serves as an excellent model for the interaction between p62

and p53 TAD2 (19, 20). In our NMR studies, we used $Tfb1_{1–115}$ as a model for $p62_{1–127}$ because of an inherent instability of $p62_{1–127}$ in solution, especially at high concentrations. Additions of $TFIIE\alpha_{336–439}$ to ^{15}N-labeled $Tfb1_{1–115}$ resulted in changes in ^{1}H and ^{15}N chemical shifts for several signals of $Tfb1_{1–115}$ in the ^{1}H-^{15}N heteronuclear single quantum coherence spectroscopy (HSQC) spectrum [supporting information (SI) Fig. 5]. These chemical shift changes indicate the formation of a $Tfb1_{1–115}$/$TFIIE\alpha_{336–439}$ complex, and they also serve to identify residues that are either directly involved in the complex formation or in close proximity to the binding interface. When mapped on the solution structure of free $Tfb1_{1–115}$, the residues displaying significant chemical shift changes cluster on a positively charged surface defined by strands β5, β6, and β7 (Fig. 1*A*). The binding site for $TFIIE\alpha_{336–439}$, as determined by NMR chemical shift mapping, is almost identical to the binding site previously observed for p53 TAD2 (Fig. 1*B*), VP16 TAD, and phosphatidylinositol 5-phosphate (PtdIns5P) (19).

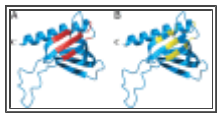

Fig. 1.

The TFIIEα carboxyl terminus binding site on Tfb1 is similar to the p53 binding site on Tfb1. (*A*) Ribbon model of the free $Tfb1_{1–115}$ (19). The amino acids showing a significant chemical shift change {$\Delta\delta_{(ppm)} > 0.15$; $\Delta\delta = [(0.17\Delta N_H)^2 + (\Delta H_N)^2]^{1/2}$} upon formation of the Tfb1/TFIIEα complex and defining the binding site of TFIIEα on Tfb1 are shown in red. (*B*) Ribbon model of the free $Tfb1_{1–115}$. The binding site for the p53 TAD2, as determined by NMR mapping studies (20), is highlighted in yellow.

TFIIEα, p53, and PtdIns5P Compete for Binding to Tfb1.

p53 TAD2 binds the PH domain of Tfb1 with a K_d of 391 ± 74 nM (20), and it appears to share a common binding site on Tfb1 with $TFIIE\alpha_{336–439}$ and PtdIns5P. To test whether p53 and $TFIIE\alpha_{336–439}$ would compete for binding to Tfb1, we performed a displacement experiment by NMR. To a sample containing ^{15}N-labeled $p53_{20–73}$ (0.5 mM) we added a substoichiometric amount of unlabeled $Tfb1_{1–115}$ (0.4 mM). As previously observed (20), addition of unlabeled $Tfb1_{1–115}$ to ^{15}N-labeled $p53_{20–73}$ produced significant changes in the ^{1}H and ^{15}N chemical shifts in the p53 spectra (Fig. 2*A*). To the sample containing the ^{15}N-$p53_{20–73}$/$Tfb1_{1–115}$ complex we then added unlabeled $TFIIE\alpha_{336–439}$ (0.5 mM), and we observed that the ^{1}H and ^{15}N resonances of ^{15}N-$p53_{20–73}$, which had shifted in the ^{15}N-$p53_{20–73}$/$Tfb1_{1–115}$ complex formation, returned to the values characteristic of the free form (*B*).

complex formation, returned to the values characteristic of the free form (Fig. 2*B*). In a similar manner, we tested whether TFIIEα$_{336–439}$ could displace PtdIns5P from its binding site on Tfb1. To a sample containing ^{15}N-Tfb1 (0.25 mM) we added PtdIns5P (0.36 mM) and observed that several residues of Tfb1 showed characteristic changes in ^{1}H and ^{15}N chemical shifts indicative of the ^{15}N-Tfb1/PtdIns5P complex formation (SI Fig. 6*A*) (19). To this sample we then added unlabeled TFIIEα$_{336–439}$ (0.36 mM). Several of the Tfb1 residues that had shown changes in chemical shift upon formation of the ^{15}N-Tfb1/PtdIns5P complex were now changing in different directions (SI Fig. 6*B*) and displayed the same chemical shift values observed for the ^{15}N-Tfb1/TFIIEα$_{336–439}$ complex (SI Fig. 5). These results clearly show that TFIIEα$_{336–439}$ competes with both p53$_{20–73}$ and PtdIns5P for the same binding site on Tfb1.

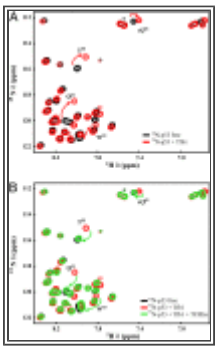

Fig. 2.

In vitro competition between p53 and TFIIEα for binding to Tfb1. (*A*) Overlay of a selected region from the two-dimensional ^{1}H-^{15}N HSQC spectra for a 0.5 mM sample of ^{15}N-labeled p53$_{20–73}$ in the free form (black) and in the presence of 0.4 mM unlabeled Tfb1$_{1–115}$ (red). (*B*) Overlay of a selected region from the two-dimensional ^{1}H-^{15}N HSQC spectra for a 0.5 mM sample of ^{15}N-labeled p53$_{20–73}$ in the free form (black), in the presence of 0.4 mM unlabeled Tfb1$_{1–115}$ (red), and after addition of 0.5 mM unlabeled TFIIEα$_{336–439}$ (green). For clarity only some of the signals that undergo significant changes in ^{1}H and ^{15}N chemical shifts upon formation of the complex with Tfb1 (*A*) and that are subsequently displaced by the addition of TFIIEα (*B*) are indicated by red and green arrows, respectively.

Structure of TFIIEα$_{336–439}$.

Because TFIIEα$_{336–439}$ is highly acidic and has an amino acid composition similar to the TADs of p53 and VP16, it seemed logical to assume that TFIIEα$_{336–439}$ would be mostly disordered in solution because this is what is observed for the TADs of both VP16 and p53 (21, 22). Surprisingly, NMR spectra revealed that TFIIEα$_{336–439}$ is not fully disordered in solution and contains a folded domain (SI Fig. 7*A*). The three-dimensional NMR structure of TFIIEα$_{336–439}$ was determined by using a set of 574 NOE-derived distance restraints, five hydrogen-bond restraints, and 91 dihedral angle restraints (SI Table 3). Several amino acids at the amino terminus (residues 336–379) of

TFIIEα$_{336–439}$ were not observed in the ^{1}H-^{15}N HSQC spectrum because of either rapid amide proton exchange at pH 7.5 and/or line broadening caused by conformational exchange. The amino terminus also showed a high degree of backbone motion on the picosecond-to-nanosecond time scale, as derived from ^{1}H-^{15}N heteronuclear NOE experiments (SI Fig. 7*B*), and this supports the presence of a flexible and disordered region localized between residues 336 and 379. For these reasons, the disordered region spanning residues 336–379 was not included in the structure calculation. A total of 50 structures was calculated, all of them satisfying the experimental constraints with no NOE violation >0.2 □ and no backbone dihedral angle violation >2°. The Ramachandran plot for the entire ensemble showed that 99.4% of the φ and ψ dihedral angles were within the most favored or allowed regions, whereas only 0.2% of the amino acids had unfavorable backbone conformations. The 20 structures with the lowest energies were selected for statistical analysis (SI Table 3).

TFIIEα$_{336–439}$ contains a small 39-residue folded domain spanning residues 395–433 arranged in a ββααα topology (Fig. 3*A* and SI Fig. 8). This fold is characterized by one short antiparallel β-sheet formed by strand β1 (residues 395–398) and strand β2 (residues 401–404) followed by three α-helices, α1 (residues 405–410), α2 (residues 412–417), and α3 (residues 420–433). The axes of helices α1 and α2 form a 60° angle and lie in a plane almost perpendicular to the β-sheet plane, whereas the third helix flanks strand β1 (Fig. 3*A*). The three helices pack together on one side of the β-sheet to form the hydrophobic core of the protein, which is stabilized by interactions involving side chains from β1 (Val^{396} and Val^{398}), β2 (Phe^{403}), α1 (Tyr^{405} and Val^{408}), α2 (L^{414} and V^{415}), and α3 (Tyr^{426} and Met^{429}) (Fig. 3*B*). The hydrophobic core serves to stabilize the folded domain and to bring the highly acidic regions between residues 380 and 393 in close proximity of helix α3 at the carboxyl terminus (Fig. 3*A* and SI Fig. 9). Despite its relatively small size, the NMR-derived structure of TFIIEα$_{336–439}$ appears to represent a previously unidentified polypeptide fold. In fact, an extensive search of the structural databases using both the Dali method (23) and the combinatorial extension method (24) failed to identify any significant matches.

Fig. 3.

The carboxyl terminus of TFIIEα contains a small folded domain. (*A*) Overlay of the 20 lowest-energy structures of the TFIIEα carboxyl terminus (residues 380–439).

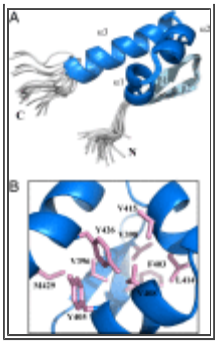

The structures were superimposed by using the backbone atoms C′, C^{α}, and N of residues 393–433. For clarity, the disordered region between residues 380 and 389 is not shown. (*B*) Ribbon representation of the lowest-energy structure of $TFIIE\alpha_{380–439}$. The side chains of the residues that are part of the hydrophobic core are highlighted in pink.

NMR Mapping Studies of the Tfb1 Binding Site on TFIIEα.

Next we performed NMR chemical shift mapping studies to define the binding site of $Tfb1_{1–115}$ on $TFIIE\alpha_{336–439}$. As observed for the $^{15}N\text{-}Tfb1_{1–115}/TFIIE\alpha_{336–439}$ complex, addition of unlabeled $Tfb1_{1–115}$ to a sample containing ^{15}N-labeled $TFIIE\alpha_{336–439}$ resulted in significant chemical shift changes for several signals in the $^{1}H\text{-}^{15}N$ HSQC spectrum of $^{15}N\text{-}TFIIE\alpha_{336–439}$ (SI Fig. 10). Again, this indicates formation of a $Tfb1_{1–115}/TFIIE\alpha_{336–439}$ complex. The most significant changes in ^{1}H and ^{15}N chemical shifts {$\Delta\delta > 0.1$ ppm; $\Delta\delta = (0.17\Delta N_H)^2 + (\Delta H_N)^2]^{1/2}$} were observed in two different regions of $^{15}N\text{-}TFIIE\alpha_{336–439}$. The first region is centered between residues 377 and 393, and a second region is localized at the very carboxyl terminus, between residues 436 and 439 (Fig. 4*A*). Both of these amino acids sequences are located in disordered regions, before (residues 377–393) and after (residues 436–439) the folded domain (Fig. 4*B*), and the two areas are near each other in three-dimensional space. The folded domain appears to serve as a bridge bringing the two unstructured regions in close proximity for p62/Tfb1 binding. Consistent with this concept, these two unstructured regions of $TFIIE\alpha_{336–439}$ are highly conserved in higher organisms (25).

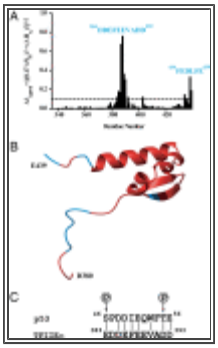

Fig. 4.

Mapping of the Tfb1 binding site on the TFIIEα carboxyl terminus. (*A*) Histogram of the variation in chemical shift [$\Delta\delta_{(ppm)}$] observed in the $^{1}H\text{-}^{15}N$ HSQC spectrum of the $^{15}N\text{-}TFIIE\alpha$ carboxyl terminus upon formation of the TFIIEα/Tfb1 complex. (*B*) Ribbon model (in red) of the lowest-energy structure for the free TFIIEα carboxyl terminus (residues 380–439). The residues showing large variations in chemical shifts [$\Delta\delta_{(ppm)} > 0.1$] in the $^{1}H\text{-}^{15}N$ HSQC spectra of $^{15}N\text{-}TFIIE\alpha$ upon formation of the TFIIEα/Tfb1 complex are mapped in blue. (*C*) Residues of p53 (46–56) that are involved in the

nteraction with the PH domain of Tfb1 are aligned with residues of TFIIEα (383–393) hat display significant chemical shift changes upon formation of the TFIIEα/Tfb1 complex. The two p53 phosphorylation sites are highlighted.

Role of F387 and F438 in the Interaction Between TFIIEα and p62.

Previous structure–function studies examining the role of TFIIE in ranscription initiation identified the acidic/hydrophobic region between esidues 377 and 393 of TFIIEα as being an important determinant for the nteraction between TFIIEα and TFIIH (7). Our ITC and NMR binding studies are in agreement with these findings; in fact, a peptide comprising the region 376–394 of TFIIEα was able to bind the PH domain of p62 with a dissociation constant of 280 ± 28 nM (Table 1). In the structure of the Tfb1/p53 complex, we determined that the hydrophobic triad Phe^{54}, Trp^{53}, and Ile^{50} makes numerous contributions to the binding interface (20). Given the fact that p53 and TFIIEα share a common binding site on Tfb/p62, we tested whether hydrophobic residues played a crucial role in TFIIEα binding to p62/Tfb1. In our NMR mapping experiments, Phe^{387} and Phe^{438} are the residues of TFIIEα undergoing the most significant chemical shift changes upon formation of the TFIIEα/Tfb1 complex (Fig. 4*A*). To investigate the role of Phe^{387} and Phe^{438} in he formation of the p62/TFIIEα complex, we performed mutational analysis and determined dissociation constants by ITC. The binding affinity for the F387A mutant is ≈20-fold lower than what is observed for the wild-type protein (Table 1), confirming that Phe^{387} is extremely important for the binding of $TFIIE\alpha_{336–439}$ to p62. On the other hand, the F438A mutant does not significantly change the binding affinity of TFIIEα for p62 (SI Table 4). However, the deletion mutant $TFIIE\alpha_{336–412}$, which is missing residues 434–439 as well as part of the folded domain, showed an increase of ≈60% in the dissociation constant (SI Table 4). We attribute this change with the $TFIIE\alpha_{336–412}$ mutant to an electrostatic contribution associated with the folded domain bringing the two acidic disordered regions in close proximity.

Surface Residues of p62 Required for Interaction with Both p53 and TFIIEα.

In previous studies we demonstrated via mutational analysis that Lys^{54} and Gln^{64} on p62 make key contributions to the binding of p62 to p53 (20). Therefore, we examined whether mutation of Lys^{54} to glutamic acid (K54E) and Gln^{64} to alanine (Q64A) significantly altered the binding of p62 to TFIIEα,

as was observed for p62 binding to p53. These two mutants were selected because they are located on the surface of p62 and they do not alter the folding properties of the PH domain of p62. ITC experiments of TFIIEα$_{336–439}$ with the two p62 mutants demonstrated that both Gln^{64} and Lys^{54} are important for the formation of the p62/TFIIEα complex; the Q64A mutation caused a 10-fold reduction in the binding affinity of p62 to TFIIEα, whereas the K54E mutation had an even more dramatic effect causing the binding constant to be reduced by >50-fold (Table 1). The effects of the K54E and Q64A mutants on the p62/TFIIEα complex are similar to those observed for the p62/p53 complex.

TFIIEα$_{336–439}$ Can Activate Transcription *in Vivo*.

Previous studies have demonstrated that, although the acid-rich carboxyl terminus of TFIIEα is not absolutely essential for basal transcription, deletion of 17 residues from residue 377 to residue 393 significantly decreased basal transcription activity (7). Given the fact that TFIIEα$_{336–439}$ shares sequence homology and a common p62/Tfb1 binding site with the TAD of p53, we investigated whether TFIIEα$_{336–439}$ was capable of activating transcription when artificially tethered to a DNA-binding domain. To verify this hypothesis, we fused TFIIEα$_{336–439}$ to the DNA-binding domain of LexA (LexA-DBD) and tested whether it could activate the transcription of a *lacZ* reporter gene in an *in vivo* yeast system. The LexA-DBD/TFIIEα$_{336–439}$ fusion protein did activate transcription *in vivo*, and the activity was ≈10-fold higher than the negative control (LexA-DBD) and ≈40-fold lower than LexA-GAL4 (Table 2). In addition, mutation of Phe^{387} to either alanine (LexA-DBD/TFIIEα$_{336–439}$ F387A) or proline (LexA-DBD/TFIIEα$_{336–439}$ F387P) resulted in an ≈66% reduction in transcription activity in the LexA system (Table 2). Similarly, mutation of Val^{390} to alanine (LexA-DBD/TFIIEα$_{336–439}$ V390A) resulted in an ≈ 50% reduction in transcription activity in the same assay (Table 2).

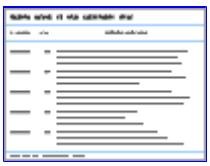

Table 2.
Transactivation by LexA fusion proteins

CONCLUSION

The general transcription factor TFIIE recruits TFIIH to the transcription

preinitiation complex by a direct interaction between its α-subunit and the p62/Tfb1 subunit of TFIIH. Despite the importance of this interaction, very little is known regarding the molecular interactions required for the formation of this complex. We have examined the molecular basis for the interaction between TFIIEα and the p62/Tfb1 subunit of TFIIH. We have determined by ITC that the acidic carboxyl terminus of TFIIEα (TFIIE$\alpha_{336–439}$) directly binds the amino-terminal PH domain of p62/Tfb1 with nanomolar affinity. NMR mapping and mutagenesis studies demonstrate that the TFIIEα binding site on p62/Tfb1 is identical to the binding site for p53 TAD2. In addition, we demonstrate that TFIIE$\alpha_{336–439}$ is capable of competing with p53 for a common binding site on p62/Tfb1 and that TFIIE$\alpha_{336–439}$ and the diphosphorylated form (pS46/pT55) of p53 TAD2 have similar binding constants. NMR structural studies reveal that TFIIE$\alpha_{336–439}$ contains a small domain (residues 395–433) folded in a novel ββααα topology. NMR mapping studies indicate that the structured region of TFIIEα serves to bring the two adjacent unstructured acidic/hydrophobic regions that are important for p62/Tfb1 binding in close proximity to one another. We also demonstrate that, like p53, TFIIE$\alpha_{336–439}$ can activate transcription *in vivo* and that the unstructured acidic/hydrophobic region of TFIIE$\alpha_{336–439}$ between residues 377 and 393 is important for this activity.

Our results clearly demonstrate that there are functional similarities between the acidic carboxyl terminus of TFIIEα and p53 TAD2. The ability of TFIIE$\alpha_{336–439}$ to function as an activator when artificially tethered to a DNA-binding domain is consistent with previous studies demonstrating that, whereas this domain is not absolutely essential for basal transcription, its presence increased the rate of transcription by 90% (7). Our studies also point to similarities between TFIIEα and p53 in binding to the p62/Tfb1 subunit of TFIIH as they compete for the same binding site on the PH domain. Comparison of several key molecular determinants required for the interaction between TFIIEα and p62/Tfb1 with those required for the interaction between p53 and p62/Tfb1 support this conclusion. The region of p53 TAD2 that binds to p62/Tfb1 is mainly disordered in the free form but forms a nine-residue α-helix between residue 47 and residue 55 when bound to Tfb1. The acidic/hydrophobic stretch between residues 377 and 395 in TFIIEα is disordered in the free form, and preliminary NMR results indicate that it becomes more ordered in the TFIIEα/Tfb1 complex (P.D.L. and J.G.O., unpublished data). A secondary structure prediction algorithm

(http://bioinf.cs.ucl.ac.uk/psipred) also predicts an α-helix between residues 379 and 390. In addition, three hydrophobic residues within the helix of p53 (Ile-50, Phe-53, and Trp-54) make crucial interactions with Tfb1 in the complex. In the case of TFIIEα, two hydrophobic residues (Phe-387 and Val-390) display the most dramatic chemical shift changes in NMR mapping studies with Tfb1, and mutation of either of these two hydrophobic residues significantly impairs the interaction of p62 with TFIIEα. Finally, specific surface residues of p62 such as Lys-54 and Gln-64 that are essential for the formation of the p53/p62 complex also play significant roles in the TFIIEα/p62 complex.

Despite the interesting similarity in the interactions leading to the formation of the p53/p62 complex and the TFIIEα/p62 complex and the fact that p53 and TFIIEα compete for binding to the same site, it appears that there are differences in the molecular determinants governing the formation of these two complexes. This is demonstrated by the fact that TFIIEα binds the PH domain of p62 ≈80-fold more tightly than does p53 TAD2. The key differences seem to involve the role of several acidic amino acids in TFIIEα surrounding the hydrophobic residues Phe-387 and Val-390. In the case of p53, diphosphorylation at Ser-46 (pS46) and Thr-55 (pT55) significantly enhances the binding of p53 to p62. The effect of the two phosphorylation events is additive, and the pS46/pT55 diphosphorylated p53 binds to p62 with an affinity similar to that with which TFIIEα binds to p62 (97 ± 33 nM versus 45 ± 25 nM). Comparison of the p53 and TFIIEα sequences demonstrates that pSer46 corresponds to Glu-383 and pThr55 corresponds to Asp-392 in TFIIEα (Fig. 4*C*). Given the fact that the two phosphorylation sites in p53 correspond to acidic residues in TFIIEα, one could propose that this is a very similar binding mechanism. These results indicate a possible interplay between p53 and TFIIEα in regulating transcription through TFIIH that could be modulated by the phosphorylation state of p53.

In conclusion, we have demonstrated that there is a strong functional relationship between the acidic carboxyl terminus of TFIIEα and the TADs of activator proteins such as p53 and VP16. The competition between p53 and TFIIEα for binding to TFIIH suggests that there is an intimate relationship between TFIIEα and activator proteins containing acidic TAD and that, in the case of p53, phosphorylation of Ser-46 and Thr-55 could be an important regulation step in the process. It is known that p53 and VP16 activate both

the initiation and elongation phases of transcription and that the ability to activate the elongation phase correlates with the fact that they interact directly with TFIIH. It is possible that VP16 and p53 activate the elongation phase of transcription competing with TFIIEα for binding to TFIIH. Future investigations are needed to address the functional and structural role of the competition between TFIIEα and transcriptional activator proteins with acidic TADs.

METHODS

Cloning of Recombinant Proteins.

The sequences encoding TFIIEα$_{336–439}$ (residues 336–439) and TFIIEα$_{336–412}$ (residues 336–412) were cloned into pGEX-2T. The GST-Tfb1$_{1–115}$ and GST-p62$_{1–127}$ were prepared as previously described (19). Site-directed mutagenesis was carried out by overlapping primers method (26) or with the QuikChange II site-directed mutagenesis kit (Stratagene). Plasmids to express the LexA-TFIIEα$_{336–439}$ fusion proteins were constructed by inserting the NcoI-BamHI-digested PCR products, which were generated by using the GST plasmids described above as templates, between the NcoI and BamHI sites of plasmid AB-426 (27). Plasmid pSH17-4 encoding the GAL4 activation domain fused to the LexA DBD has been described (27).

Protein Expression and Purification.

The PH domains of Tfb1 (residues 1–115), p62 (residues 1–127), and mutants were expressed and purified as previously described (19). TFIIEα$_{336–439}$ and mutants were expressed as a GST fusion protein in *Escherichia coli* host strain TOPP2 and bound to GSH resin. The resin-bound protein was incubated overnight with thrombin (Calbiochem). After cleavage, the supernatant was purified by FPLC over a Q-Sepharose High Performance column (Amersham Pharmacia).

Peptide Synthesis.

A synthetic peptide containing residues 376–394 plus an amino-terminal tyrosine residue (TFIIEα$_{376–394}$) for quantification at A_{280} was purchased from the Sheldon Biotechnology Centre (McGill University) and purified by HPLC.

Isothermal Titration Calorimetry Studies.

The ITC titration experiments were performed as previously described (28) in 20 mM Tris or in 20 mM Tris/100 mM NaCl buffer at pH 7.5. All titrations fit

the single binding site mechanism with 1:1 stoichiometry.

NMR Samples.

The samples for structural studies of the free TFIIEα$_{336–439}$ contained 1 mM protein (^{15}N- or ^{15}N/^{13}C-labeled) in 20 mM sodium phosphate (pH 7.5), 200 mM NaCl, 1 mM EDTA (NMR buffer), and 90% H_2O/10% D_2O or 99.9% D_2O. For the NMR mapping we used two samples in NMR buffer. One sample contained 0.5 mM ^{15}N-Tfb1$_{1–115}$, and unlabeled TFIIEα$_{336–439}$ was added to a final ratio of 1:1. The second sample consisted of 0.5 mM ^{15}N-TFIIEα$_{336–439}$, and unlabeled Tfb1 was added to a final ratio of 1:1.

For the p53 displacement experiment we used a sample containing 0.5 mM ^{15}N-labeled p53$_{20–73}$ in NMR buffer. To this sample unlabeled Tfb1$_{1–115}$ was added to a final concentration of 0.4 mM. Then in a second addition we titrated in unlabeled TFIIEα$_{336–439}$ to a final concentration of 0.5 mM. For the PtdIns5P displacement experiment we used a sample containing 0.25 mM ^{15}N-labeled Tfb1$_{1–115}$ in 15 mM Tris (pH 7.0), 200 mM NaCl, 1 mM EDTA, and 90% H_2O/10% D_2O. To this sample we added PtdIns(5)P (Echelon) to a final concentration of 0.36 mM. Then in a second addition we titrated in unlabeled TFIIEα$_{336–439}$ to a final concentration of 0.36 mM.

NMR Spectroscopy.

NMR experiments were carried out at 300 K on Varian Unity Inova 500-, 600-, and 800-MHz spectrometers. The backbone and aliphatic side chain resonances (^{1}H, ^{15}N, and ^{13}C) were assigned by triple resonance experiments [HNCO, HNCACB, (HB)CBCA(CO)NNH, C(CO)NNH, H(CCO)NNH, HCCH-COSY, and HNHA]. Interproton distance restraints were derived from ^{15}N-edited NOESY-HSQC and ^{13}C-edited HMQC-NOESY spectra (τ_m = 90 ms). The NMR data were processed with NMRPipe/NMRDraw (29) and analyzed with NMRView (30).

Structures Calculation.

The NOE-derived distance restraints were divided into three classes defined as strong (1.8–2.8 □), medium (1.8–3.4 □), and weak (1.8–5.0 □). Backbone dihedral angles were derived with the program TALOS (31) and from the values of the coupling constants $^3J_{HNHA}$ (32). After exchange in D_2O, slowly exchanging amide protons were identified by recording a ^{1}H-^{15}N HSQC spectrum of TFIIEα$_{336–439}$. The five hydrogen-bond restraints derived from the slowly exchanging amide protons were used only for the amide protons

in elements of secondary structure and for which the proton acceptor could be easily identified based on the preliminary structure. The structures of TFIIE$\alpha_{336–439}$ were calculated with the program CNS by using a combination of torsion angle and Cartesian dynamics (33) and starting from one extended structure with standard geometry. The protocol used the conformational database potential derived from structural databases (34). The structures were assessed by using PROCHECK-NMR (35) and MOLMOL (36). The figures were generated with MOLMOL (36) and PyMol (www.pymol.org).

Liquid Culture Assay to Measure β-Galactosidase.

Yeast strains were transformed with the LexA operator–*lacZ* fusion plasmid pSH18–34 (eight LexA-binding sites) and various LexA-fusion proteins to determine the relative abilities of the fusion proteins to activate transcription in the yeast model system. In all cases, cells were grown to mid-logarithmic phase in growth media lacking Ura and His. The number of cells used for the various LexA fusion proteins was adjusted to obtain reliable readings of optical density at 420 nm. For each measurement, β-galactosidase activity was determined from three independent cultures and average values are given. One unit of β-galactosidase is defined as the amount that hydrolyzes 1 μmol of ONPG to *o*-nitrophenol and galactose per minute per cell (37).

SUPPLEMENTARY MATERIAL

Supporting Information

Click here to view.

ACKNOWLEDGMENTS.

This work was supported by National Cancer Institute of Canada Grant 016302 with funds from the Terry Fox Foundation (to J.G.O.), Canadian Institutes of Health Research Grant (CIHR) MOP-74739, and CIHR Grant 117713 (to P.L.). P.D.L. is the recipient of a postdoctoral fellowship from the CIHR. P.L. is a Canadian Research Chair in Structural Biology of RNA. The NOESY experiment at 800 MHz was recorded at the Québec/Eastern Canada High Field NMR Facility, which is supported by grants from the Canada Foundation for Innovation.

FOOTNOTES

The authors declare no conflict of interest.

This article is a PNAS Direct Submission.

Data deposition: The atomic coordinates for TFIIE$\alpha_{336–439}$ have been deposited in the Protein Data Bank, www.pdb.org (PDB ID code 2JTX).

This article contains supporting information online at www.pnas.org/cgi/content/full/0707892105/DC1.

REFERENCES

1. Kodandapani R, Pio F, Ni C-Z, Piccialli G, Klemsz MJ, McKercher SR, Maki RA, Ely KR. *Nature.* 1996;**380**:456–460. [PubMed]

2. Hampsey M. *Microbiol Mol Biol Rev.* 1998;**62**:465–503. [PMC free article] [PubMed]

3. Flores O, Lu H, Reinberg D. *J Biol Chem.* 1992;**267**:2786–2793. [PubMed]

4. Maxon ME, Goodrich JA, Tjian R. *Genes Dev.* 1994;**8**:515–524. [PubMed]

5. Lu H, Flores O, Weinmann R, Reinberg D. *Proc Natl Acad Sci USA.* 1991;**88**:10004–10008. [PMC free article] [PubMed]

6. O'Brien T, Hardin S, Greenleaf A, Lis JT. *Nature.* 1994;**370**:75–77. [PubMed]

7. Ohkuma Y, Hashimoto S, Wang CK, Horikoshi M, Roeder RG. *Mol Cell Biol.* 1995;**15**:4856–4866. [PMC free article] [PubMed]

8. Kuldell NH, Buratowski S. *Mol Cell Biol.* 1997;**17**:5288–5298. [PMC free article] [PubMed]

9. Ohkuma Y, Roeder RG. *Nature.* 1994;**368**:160–163. [PubMed]

10. Okamoto T, Yamamoto S, Watanabe Y, Ohta T, Hanaoka F, Roeder RG, Ohkuma Y. *J Biol Chem.* 1998;**273**:19866–19876. [PubMed]

11. Tirode F, Busso D, Coin F, Egly JM. *Mol Cell.* 1999;**3**:87–95. [PubMed]

12. Lu H, Zawel L, Fisher L, Egly JM, Reinberg D. *Nature.* 1992;**358**:641–645. [PubMed]

13. Kobor MS, Greenblatt J. *Biochim Biophys Acta.* 2002;**1577**:261–275. [PubMed]

14. Drapkin R, Reardon JT, Ansari A, Huang J-C, Zawel L, Ahn K, Sancar A, Reinberg D. *Nature.* 1994;**368**:769–772. [PubMed]

15. Yankulov KY, Bentley DL. *EMBO J.* 1997;**16**:1638–1646. [PMC free article] [PubMed]

16. Bushnell DA, Bamdad C, Kornberg RD. *J Biol Chem.* 1996;**271**:20170–20174. [PubMed]

17. Zhu J, Zhou W, Jiang J, Chen X. *J Biol Chem.* 1998;**273**:13030–13036. [PubMed]

18. Kato S, Han SY, Liu W, Otsuka K, Shibata H, Kanamaru R, Ishioka C. *Proc Natl Acad Sci USA.* 2003;**100**:8424–8429. [PMC free article] [PubMed]

19. Di Lello P, Nguyen BD, Jones T, Potempa K, Kobor MS, Legault P, Omichinski JG. *Biochemistry.* 2005;**44**:7678–7686. [PubMed]

20. Di Lello P, Miller Jenkins LM, Jones TN, Nguyen BD, Hara T, Yamaguchi H, Dikeakos JD, Appella E, Legault P, Omichinski JG. *Mol Cell.* 2006;**22**:731–740. [PubMed]

21. O'Hare P, Williams G. *Biochemistry.* 1992;**31**:4150–4156. [PubMed]

22. Lee H, Mok KH, Muhandiram R, Park K-H, Suk J-E, Kim D-H, Chang J, Sun YC, Choi KY, Han K-H. *J Biol Chem.* 2000;**275**:29426–29432. [PubMed]

23. Holm L, Sander C. *J Mol Biol.* 1993;**233**:123–138. [PubMed]

24. Shindyalov IN, Bourne PE. *Protein Eng.* 1998;**11**:739–747. [PubMed]

25. Yamamoto S, Watanabe Y, van der Spek PJ, Watanabe T, Fujimoto H, Hanaoka F, Ohkuma Y. *Mol Cell Biol.* 2001;**21**:1–15. [PMC free article] [PubMed]

26. Higuchi R, Krummel B, Saiki RK. *Nucleic Acids Res.* 1988;**16**:7351–7367. [PMC free article] [PubMed]

27. Ausubel FM, Brent R, Kingston RE, Moore DD, Smith JA, Struhl K. *Current Protocols in Molecular Biology.* New York: Wiley; 1997.

28. Houtman JCD, Higashimoto Y, Dimasi N, Cho S, Yamaguchi H, Bowden B, Regan C, Malchiodi EL, Mariuzza R, Schuck P, et al. *Biochemistry.* 2004;**43**:4170–4178. [PubMed]

29. Delaglio F, Grzesiek S, Vuister GW, Zhu G, Pfeifer J, Bax A. *J Biomol NMR.* 1995;**6**:277–293. [PubMed]

30. Johnson BA, Blevins RA. *J Biomol NMR.* 1994;**4**:603–614.

31. Cornilescu G, Delaglio F, Bax A. *J Biomol NMR.* 1999;**13**:289–302. [PubMed]

32. Vuister GW, Bax A. *J Am Chem Soc.* 1993;**115**:7772–7777.

33. Brunger AT, Adams PD, Clore GM, Gros P, Grosse-Kunstleve RW, Jiang J-S, Kuszewski J, Nilges M, Pannu NS, Read RJ, et al. *Acta Crystallogr D.* 1998;**54**:905–921. [PubMed]

34. Kuszewski J, Gronenborn AM, Clore GM. *Protein Sci.* 1996;**5**:1067–1080. [PMC free article] [PubMed]

35. Laskowski RA, Antoon J, Rullmann C, Macarthur MW, Kaptein R, Thornton JM. *J Biomol NMR.* 1996;**8**:477–486. [PubMed]

36. Koradi R, Billeter M, Wüthrich K. *J Mol Graphics.* 1996;**14**:51–55.

37. Miller JH. *A Short Course in Bacterial Genetics.* Plainview, NY: Cold Spring Harbor Lab Press; 1992.